Society of Medical Education & Research

2025, Volume 5, Issue 1, Page No: 179-199
ISSN: 3108-4834

Archive of International Journal of Cancer and Allied Science

EFNB2/EPHB4 Axis Activation Promotes Post-Metastatic Colonization of Colorectal Cancer in the Liver through LDLR-Mediated Cholesterol Metabolism

Alina Ioana Pop[1]*, Raluca Daniela Stan[1]

[1]Institute of Oncology "Prof. Dr. Ion Chiricuta", Cluj-Napoca, Romania.

***E-mail** ✉ a.pop.ioicn@yahoo.com

Abstract

The microenvironment of distant organs plays a critical role in modulating tumor metastasis; however, the molecular interactions between metastatic cancer cells and their target organs remain poorly understood. In this study, we identified a marked upregulation of EFNB2 expression in colorectal cancer (CRC) liver metastases (LM), whereas no such increase was observed in pulmonary metastases (PM) or primary CRC tumors. Functional analyses demonstrated that EFNB2 exerts a pro-tumorigenic effect in CRC liver metastasis both in vitro and in vivo. Mechanistically, EFNB2 promotes metastatic growth through forward signaling by engaging the EPHB4 receptor. Activation of the EFNB2–EPHB4 signaling axis enhances low-density lipoprotein receptor (LDLR)–mediated cholesterol uptake in CRC liver metastases. Furthermore, this axis upregulates LDLR transcription by modulating STAT3 phosphorylation. Genetic or pharmacological inhibition of LDLR abrogated the tumor-promoting effects of the EFNB2–EPHB4 pathway in CRC liver metastasis. Analysis of clinical datasets revealed that CRC patients with liver metastases exhibiting high EFNB2 expression had significantly reduced survival compared with those displaying low EFNB2 levels. Consistently, blockade of the EFNB2–EPHB4 axis significantly extended survival in BALB/c nude mice bearing CRC liver metastases under a high-cholesterol diet. Collectively, these findings uncover a critical mechanism by which the EFNB2–EPHB4 axis regulates cholesterol uptake and drives the progression of colorectal cancer liver metastases.

Keywords: Cholesterol metabolism, Colorectal cancer, Tumor metastasis, Liver metastases

Introduction

Colorectal cancer (CRC) is among the most prevalent malignant tumors worldwide. According to recent epidemiological data, CRC ranks third in both incidence and mortality rates. The presence of distant metastases, particularly liver metastases (LM) and pulmonary metastases (PM), represents a major independent predictor of poor prognosis [1, 2].

Metastasis is a complex, multistep process that involves invasion of tumor cells at the primary site, survival of circulating tumor cells, colonization at distant sites, and subsequent formation of secondary tumors [3, 4]. Metastasized tumors often acquire genetic alterations compared with their primary counterparts. Although numerous genes are implicated in cancer metastasis, the pro-metastatic effects of these molecules do not necessarily exhibit specificity for particular target organs. Emerging evidence shows that different breast cancer cell lines exhibit distinct preferences for metastatic sites [5]. Similarly, recent studies have revealed substantial differences in gene expression between CRC metastases at different target organs [6]. Disseminated tumor cells frequently express specific genes that enhance their ability to adapt to the microenvironment of the target organ [7]. Among CRC metastases, the liver represents the most common site of distant dissemination [8, 9], with more than 50% of patients developing LM during the course of disease. Despite advances in diagnostic and therapeutic strategies,

Access this article online https://smerpub.com/

Received: 23 February 2025; **Accepted:** 21 May 2025

How to cite this article: Pop AI, Stan RD. EFNB2/EPHB4 Axis Activation Promotes Post-Metastatic Colonization of Colorectal Cancer in the Liver through LDLR-Mediated Cholesterol Metabolism. Arch Int J Cancer Allied Sci. 2025;5(1):179-99. https://doi.org/10.51847/Z45KOBSjYh

fewer than 10% of CRC patients with LM survive beyond five years [10]. Currently, no therapeutic approaches specifically target liver metastases, highlighting the importance of understanding the molecular mechanisms underlying CRC growth in the liver, which could inform the development of more precise therapies against CRC LM.

Axon guidance factors are critical molecules in embryonic development, guiding axonal growth and the establishment of neural circuits [11-13]. These molecules are classified into four families: Semaphorins-Plexins, Netrins-DCC/UNCs, Slits-Robos, and Ephrins-Ephs. Recent evidence suggests that axon guidance factors also play important roles in tumorigenesis [14]. Several members, including SLITs and SEMAs, have been shown to influence malignant behaviors in tumor cells [15, 16]. However, their role and underlying mechanisms in CRC liver metastases remain largely unexplored.

In the present study, we investigated whether specific genes exhibit altered expression in CRC LM due to adaptation to the liver microenvironment. Through data analysis, we identified EFNB2 as significantly upregulated in LM. Mechanistically, the EFNB2/EPHB4 axis was found to promote LDLR-mediated cholesterol uptake, ultimately facilitating the colonization and growth of CRC liver metastases.

Results and Discussion

Specific upregulation of EFNB2 in CRC liver Metastases promotes post-metastatic growth

To identify gene signatures specifically associated with colorectal cancer (CRC) metastasis to the liver rather than the lung, we analyzed the GSE6988 (CRC PM) and GSE41258 (CRC LM) datasets. This analysis revealed a subset of genes upregulated exclusively in CRC liver metastases, among which EFNB2, an axon guidance molecule, emerged as a candidate of interest **(Figures 1a–e).** Immunohistochemical (IHC) analysis confirmed that EFNB2 was markedly elevated in paired CRC liver metastasis tissues, whereas its expression in primary CRC tissues did not differ significantly from adjacent noncancerous tissues **(Figure 1f).**

To validate the dynamic expression of EFNB2, we employed three experimental CRC models **(Figures 1g and h):** an orthotopic tumor model, a liver metastasis model via spleen injection, and a pulmonary metastasis model via tail vein injection. EFNB2 expression remained largely unchanged over time in tumor tissues from the orthotopic and pulmonary metastasis models **(Figures 1i and j).** In contrast, EFNB2 levels progressively increased in liver metastasis tissues over time **(Figure 1k)**. These findings suggest that upregulation of EFNB2 is specifically associated with the growth of CRC in the liver.

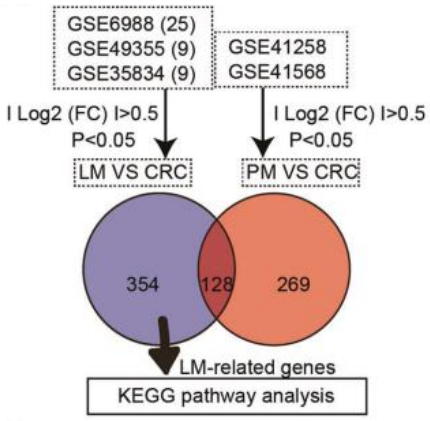

a)

GeneRatio	*P* value
Glycine, serine and threonine metabolism	1. 24E−07
Carbon metabolism	1. 61E−07
Biosynthesis of amino acids	4. 07E−06
Glyoxylate and dicarboxylate metabolism	3. 53E−05
Phenylalanine metabolism	3. 98E−04
Cysteine and methionine metabolism	2. 66E−03
beta-Alanine metabolism	4. 16E−03
Cholesterol metabolism	4. 24E−03
Axon guidance	9. 57E−03

b)

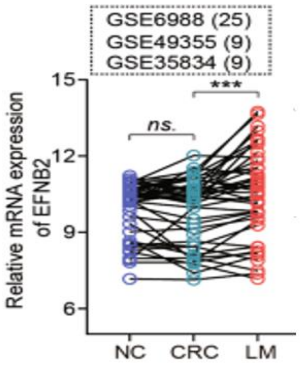
GSE6988 (25)
GSE49355 (9)
GSE35834 (9)
Relative mRNA expression of EFNB2
ns.
***
NC
CRC
LM

c)

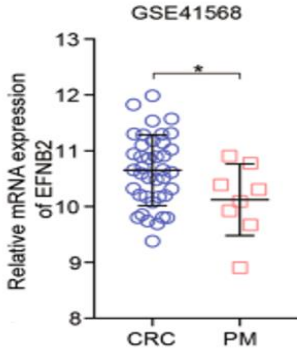
GSE41568
Relative mRNA expression of EFNB2
*
CRC
PM

d)

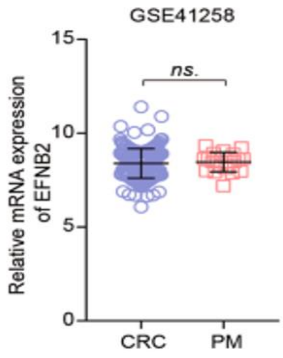
GSE41258
Relative mRNA expression of EFNB2
ns.
CRC
PM

e)

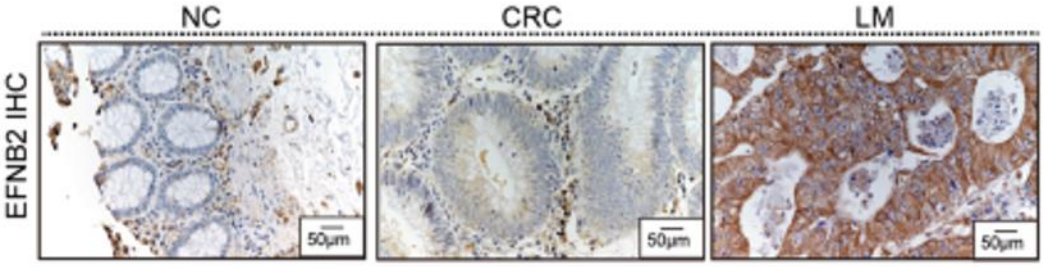
NC
CRC
LM
EFNB2 IHC
50μm

f)

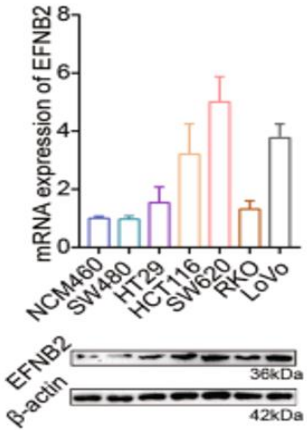
mRNA expression of EFNB2
NCM460
SW480
HT29
HCT116
SW620
RKO
LoVo
EFNB2
β-actin
36kDa
42kDa

g)

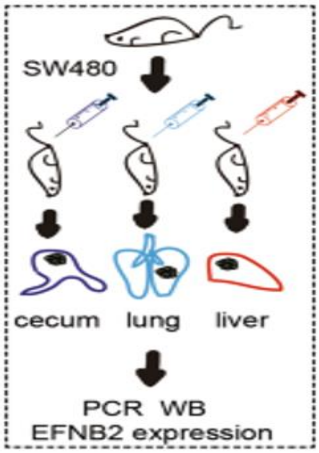
SW480
cecum
lung
liver
PCR WB
EFNB2 expression

h)

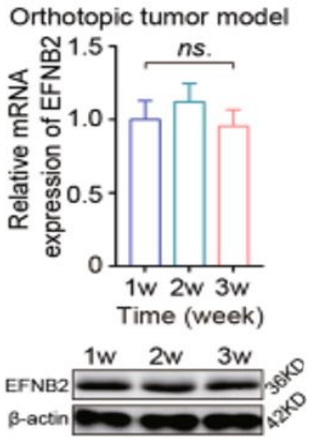
Orthotopic tumor model
Relative mRNA expression of EFNB2
ns.
1w 2w 3w
Time (week)
EFNB2
β-actin
36KD
42KD

i)

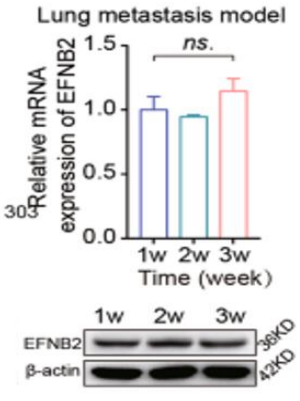
Lung metastasis model
Relative mRNA expression of EFNB2
ns.
1w 2w 3w
Time (week)
EFNB2
β-actin
36KD
42KD

j)

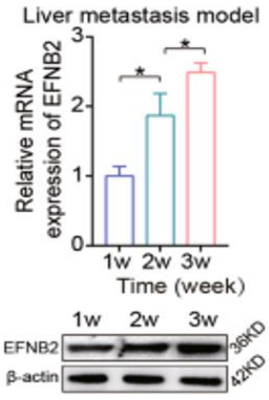
Liver metastasis model
Relative mRNA expression of EFNB2
*
*
1w 2w 3w
Time (week)
EFNB2
β-actin
36KD
42KD

k)

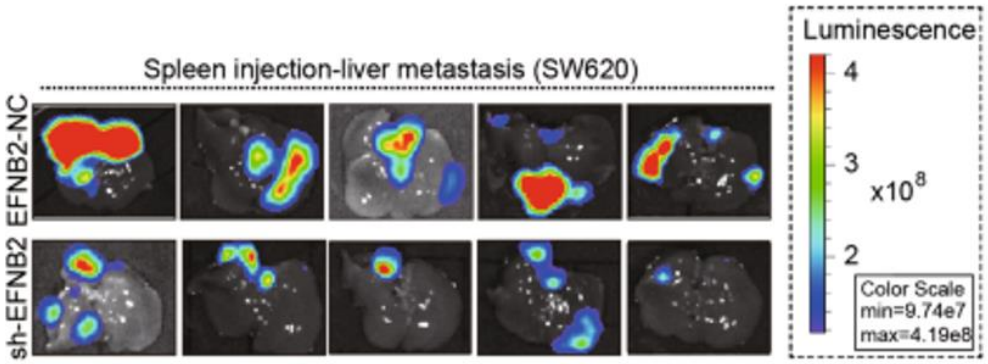

l)

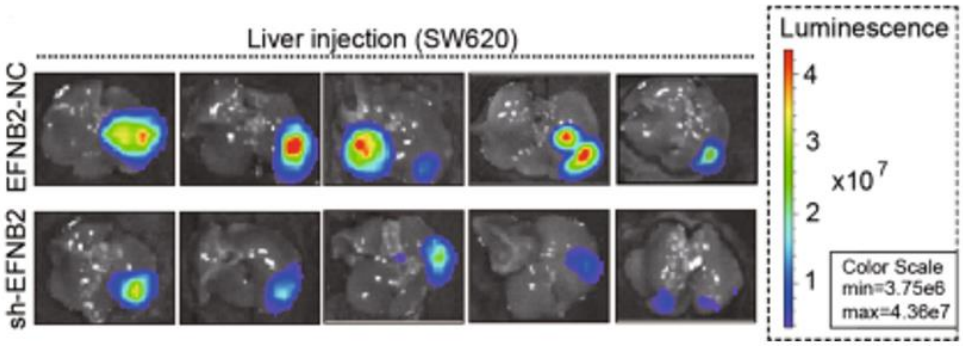

m)

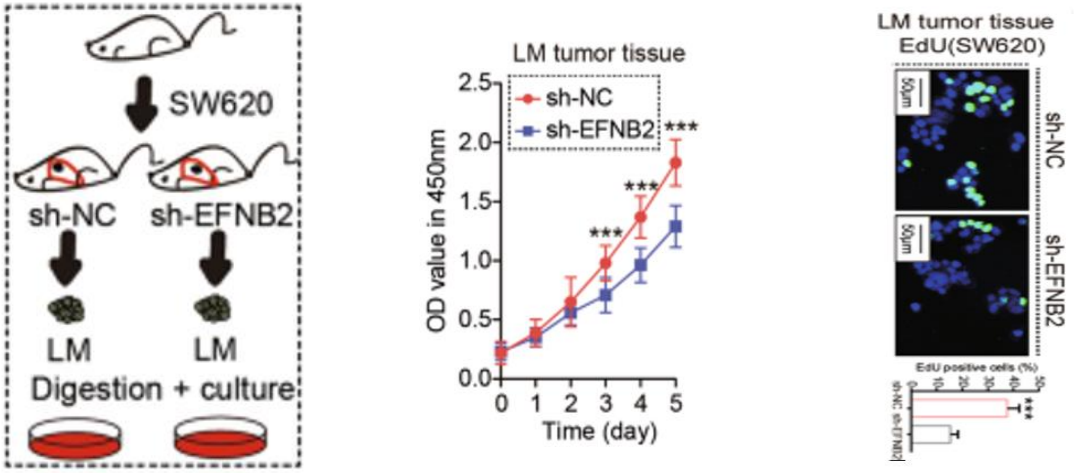

n) o) p)

Figure 1. Elevated EFNB2 expression drives post-metastatic growth of CRC liver metastases

a Genes upregulated specifically in CRC LM were identified from GSE6988, GSE49355, and GSE35834 datasets, whereas GSE41568 and GSE41258 datasets were used for CRC PM analysis. **b** KEGG pathway enrichment of genes upregulated in CRC LM. **c** EFNB2 mRNA levels in NC, LM and CRC samples from GSE6988, GSE49355, and GSE35834. **d** EFNB2 mRNA expression in CRC and PM samples from GSE41568. **e** EFNB2 mRNA expression in CRC and PM samples from GSE41258. **F** EFNB2 protein levels in paired NC, CRC, and LM tissues (n = 15 per group), scale bar: 50 μm. **g** EFNB2 mRNA and protein expression in NCM460 and six CRC cell lines. **h** Experimental models including orthotopic tumors, liver metastasis via spleen injection, and lung metastasis via tail vein injection using SW480 cells in nude mice. **i** EFNB2 mRNA and protein

expression in orthotopic tumors over 1–3 weeks (n = 6). **j** EFNB2 expression in lung metastasis tumors over 1–3 weeks (n = 6). **k** EFNB2 expression in liver metastasis tumors over 1–3 weeks (n = 6). **l** Imaging of spleen-injected liver metastasis model with sh-EFNB2 or sh-NC SW620Luc cells (n = 6), scale bar: 9.74×10^7–4.19×10^8. **m** Imaging of intrahepatic tumor model after liver injection with sh-NC SW620Luc or sh-EFNB2 cells (n = 5 per group), scale bar: 3.75×10^6–4.36×10^7. **n** LM tumor tissues from sh-EFNB2 or sh-NC mice were digested and cultured. **o** Viability of LM-derived SW620 cells assessed by CCK-8 assay. **p** Proliferation of LM-derived SW620 cells assessed by EdU assay, scale bar: 50 μm. Experiments were performed in triplicate. Data are presented as mean ± SD. Statistical significance was calculated using Student's t-tests. Ns, no statistical difference; *p < 0.05; ***p < 0.001.

Migration assays indicated that EFNB2 knockdown had minimal effect on cell motility (**Figures 1a and b**). To evaluate EFNB2's functional role in sh-NC, CRC LM or sh-EFNB2 SW620 cells were injected into the spleens of nude mice. EFNB2 depletion resulted in a marked reduction in liver tumor burden (**Figures**. **1l and 1c**). Direct intrahepatic injection of sh-NC or sh-EFNB2 cells confirmed that EFNB2 knockdown significantly impaired tumor growth in the liver (**Figures**. **1m and 1d**). Digested LM tumor tissues were cultured (**Figure 1n**), and subsequent EdU and CCK-8 assays showed that EFNB2 knockdown strongly inhibited proliferation of CRC LM cells in vitro (**Figures**. **1o and p**). Collectively, these findings indicate that EFNB2 facilitates colonization and expansion of CRC liver metastases.

EFNB2 promotes post-metastatic CRC LM growth through forward signaling

Ephrin–Eph interactions are bidirectional. Eph receptors act as classical receptors transmitting forward signaling, whereas Ephrin ligands can initiate reverse signaling when acting on Eph receptors (**Figure 2a**). To dissect the contribution of each pathway, we generated EFNB2 constructs with C-terminal truncations (ΔC + H EFNB2 and ΔC EFNB2) to block reverse signaling, and an N-terminal truncation (ΔE EFNB2) to disrupt forward signaling (**Figures 2b and 2c**). SW480 cells expressing full-length EFNB2 (EFNB2 FL) exhibited significantly higher metastatic tumor burden than cells with empty vector. Cells expressing ΔC + H EFNB2 or ΔC EFNB2 showed tumor burdens comparable to EFNB2 FL, indicating that reverse signaling is not required for promoting CRC LM growth (**Figures**. **2d and 2a**). In contrast, ΔE EFNB2-expressing cells failed to enhance post-metastatic growth relative to controls (**Figures**. **2d and 2a).**

These results were corroborated in vitro (**Figures**. **2e and 2g**), and purified protein from ΔC + H EFNB2 cells significantly increased CRC cell viability (**Figures. 2f, h and 2c**). Altogether, these data demonstrate that EFNB2 drives post-metastatic growth of CRC liver metastases predominantly through forward signaling, whereas reverse signaling is dispensable.

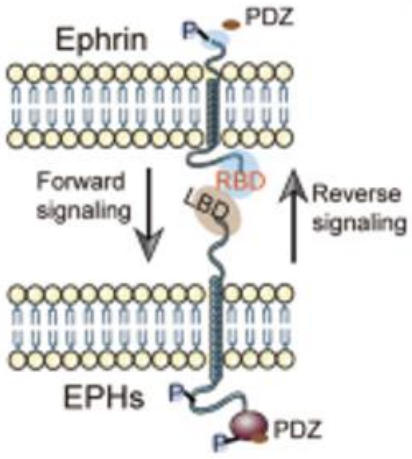

a)

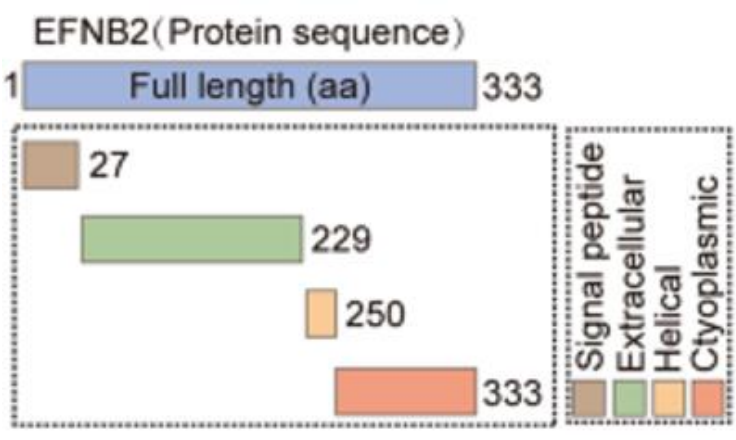

b)

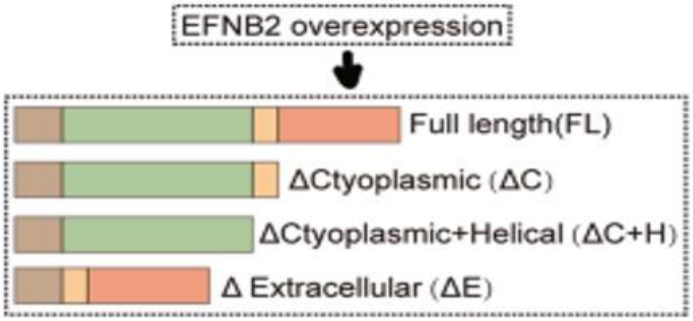
EFNB2 overexpression
Full length(FL)
ΔCtyoplasmic (ΔC)
ΔCtyoplasmic+Helical (ΔC+H)
Δ Extracellular (ΔE)

c)

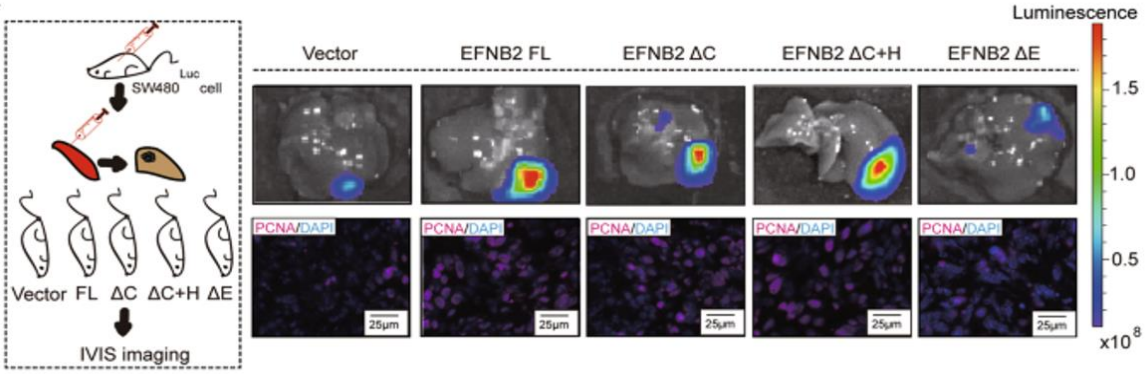
Luc
SW480 cell
Vector FL ΔC ΔC+H ΔE
IVIS imaging
Vector
EFNB2 FL
EFNB2 ΔC
EFNB2 ΔC+H
EFNB2 ΔE
Luminescence
1.5
1.0
0.5
x10^8
PCNA/DAPI
25μm

d)

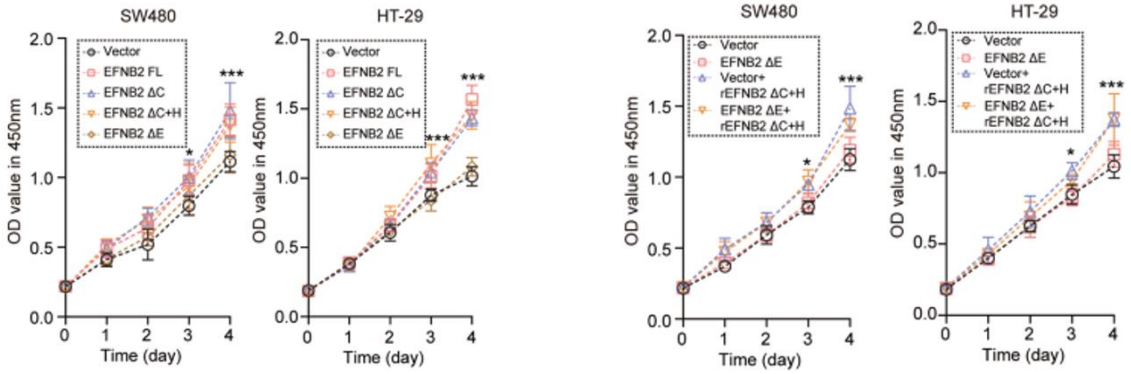
SW480
HT-29
Vector
EFNB2 FL
EFNB2 ΔC
EFNB2 ΔC+H
EFNB2 ΔE
Vector+ rEFNB2 ΔC+H
EFNB2 ΔE+ rEFNB2 ΔC+H
OD value in 450nm
Time (day)
*
***

e) f)

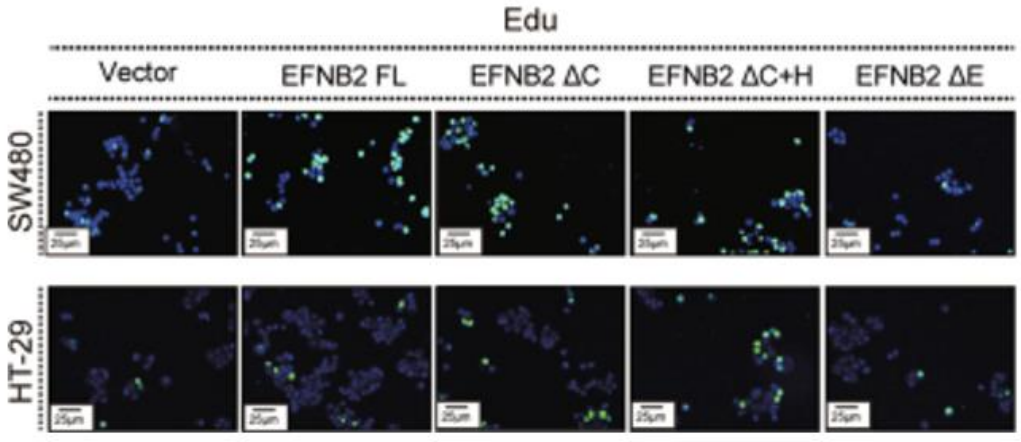
Edu
Vector
EFNB2 FL
EFNB2 ΔC
EFNB2 ΔC+H
EFNB2 ΔE
SW480
HT-29
25μm

g)

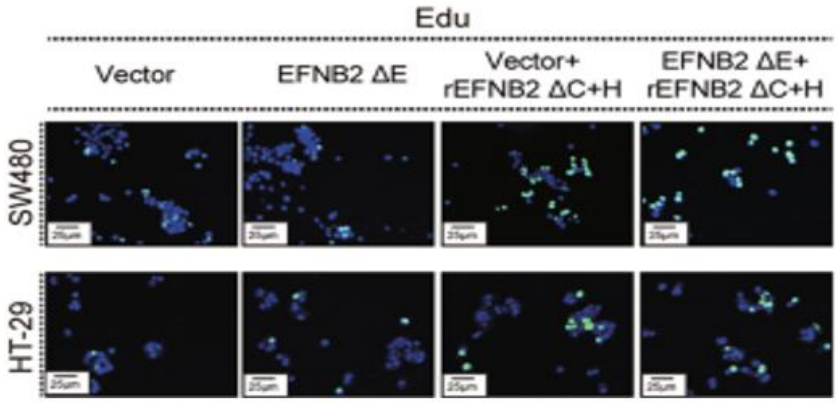

h)

Figure 2. Forward signaling through EFNB2, but not reverse signaling, supports tumor expansion following colorectal cancer liver metastasis (CRC LM).

a. Diagram depicting the directions of signal transmission. **b.** Domain architecture of the EFNB2 protein. **c.** Development of four EFNB2 overexpression vectors: full-length EFNB2 (FL), a C-terminal truncated version (EFNB2 ΔC), a C-terminal truncated version with a His-tag (EFNB2 ΔC + H), and a construct expressing only the extracellular domain (EFNB2 ΔE). **d.** Establishment of a liver metastasis model through splenic injection of SW480Luc cells expressing control vector, EFNB2 FL, EFNB2 ΔC, EFNB2 ΔC + H, or EFNB2 ΔE (n = 6 mice/group). Tumor development was tracked via bioluminescence imaging, with PCNA immunostaining performed on metastatic liver tissues (Blue: DAPI; Purple: PCNA). Scale bar: 25 μm. **e.** Assessment of cell proliferation in SW480 and HT29 lines transfected with control vector, EFNB2 FL, EFNB2 ΔC, EFNB2 ΔC + H, or EFNB2 ΔE using CCK-8 assays. **f.** Proliferation analysis via CCK-8 in SW480 and HT29 cells transfected with control vector, vector plus recombinant EFNB2 ΔC + H, EFNB2 ΔE, or EFNB2 ΔE plus recombinant EFNB2 ΔC + H. **G.** Proliferation measured by EdU incorporation in HT29 and SW480 cells expressing control vector, EFNB2 ΔC, EFNB2 FL, EFNB2 ΔE or EFNB2 ΔC + H. **h.** EdU incorporation in SW480 and HT29 cells under conditions of control vector, EFNB2 ΔE, vector plus recombinant EFNB2 ΔC + H, or EFNB2 ΔE plus recombinant EFNB2 ΔC + H. Scale bar: 25 μm. In vitro assays were repeated three times. Results are shown as mean ± SD. Comparisons were made using Student's t-tests. ns, not significant; *$p < 0.05$; ***$p < 0.001$.

The EFNB2/EPHB4 pathway facilitates outgrowth of colorectal cancer liver metastases after establishment

EFNB2 typically binds to EPH family receptors to activate intracellular signaling. Analysis of EPH receptor mRNA levels in CRC liver metastases from the GSE6988 dataset revealed selective upregulation of EPHB4 in metastatic lesions relative to primary tumors (**Figure 3a**). Functional studies in vitro confirmed that EFNB2 increased CRC cell proliferation exclusively via EPHB4, with no effect observed through other receptors tested (EPHB1, EPHB2, EPHB3, EPHB6, EPHA4) (**Figures**. **3b and 3a**).

EPHB4, a tyrosine kinase receptor, relays signals through autophosphorylation. The selective inhibitor NVP-BHG712, which targets EPHB4 kinase activity, effectively abolished EFNB2-driven cell proliferation in EdU assays (**Figures**. **3c and 3g**).

In vivo validation involved splenic injection of EFNB2-overexpressing or control SW480Luc cells into nude mice to model liver metastasis, or direct intrahepatic injection. Pharmacological (NVP-BHG712) or genetic (siRNA) inhibition of EPHB4 markedly diminished the growth advantage conferred by EFNB2 in both settings (**Figures 3d and e**). Consistent with this, PCNA immunostaining demonstrated that EPHB4 suppression counteracted EFNB2-induced proliferation in metastatic and orthotopic tumors (**Figures**. **3f, g and 3h, i**).

Metastatic liver tumors were harvested, enzymatically dissociated, and placed in culture (**Figure 3h**). Ex vivo proliferation assays (CCK-8 and EdU) verified that EFNB2 overexpression robustly enhanced growth of cells derived from liver metastases (**Figures 3i and j**).

Taken together, these results establish that EFNB2 drives colorectal cancer liver metastasis progression through direct activation of EPHB4.

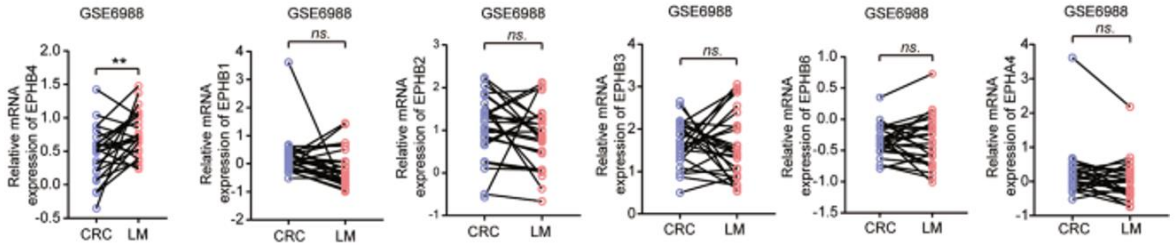

a)

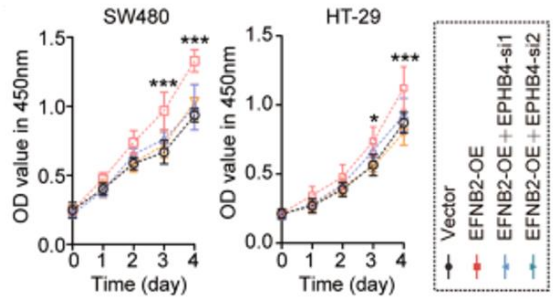

b)

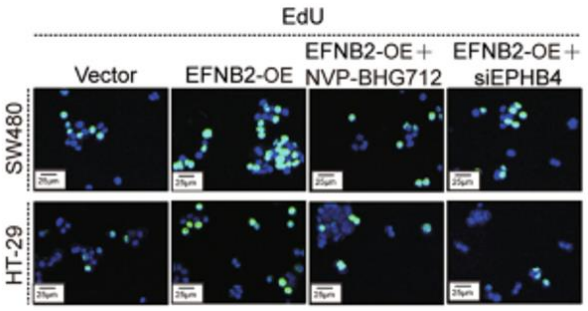

c)

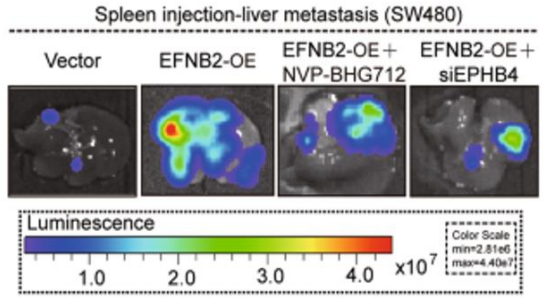

d)

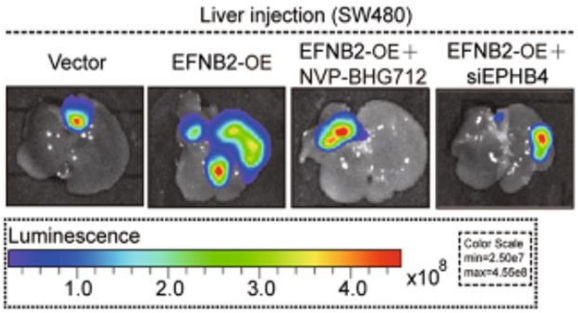

e)

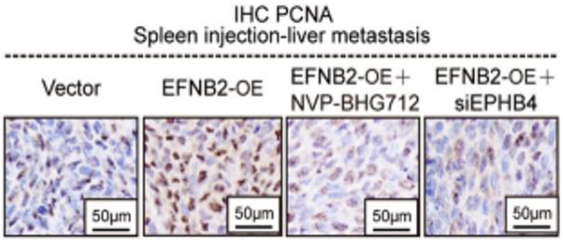

f)

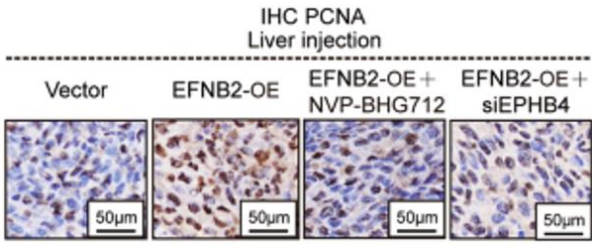

g)

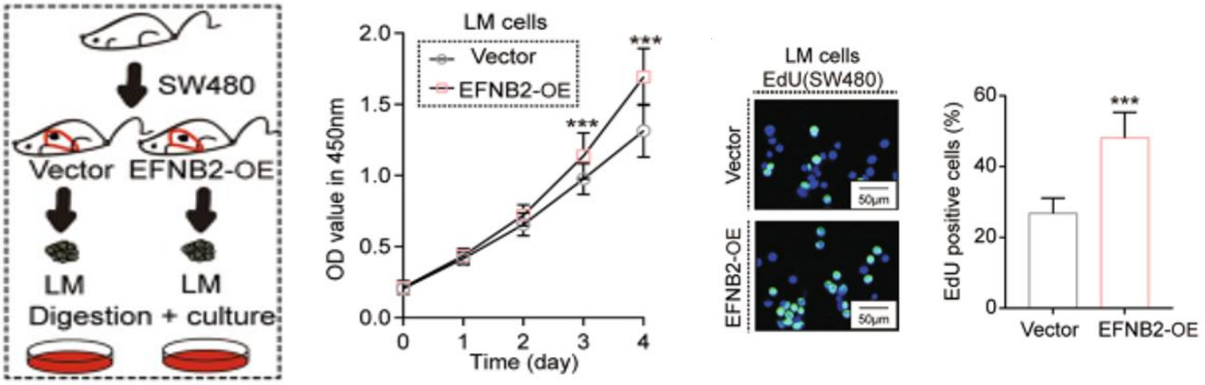

h) i) j)

Figure 3. Activation of EPHB4 by EFNB2 promotes outgrowth of established colorectal cancer liver metastases (CRC LM).

a. Expression of EPHB4 and additional EPH receptor mRNAs in primary colorectal tumors versus paired liver metastases, based on the GSE6988 dataset. **b.** Growth curves from CCK-8 assays for SW480 and HT29 cells expressing empty vector, EFNB2 overexpression (EFNB2-OE), or EFNB2-OE plus EPHB4-specific siRNA (siEPHB4). **c.** EdU-based proliferation analysis in SW480 and HT29 cells under conditions of empty vector, EFNB2-OE, EFNB2-OE combined with siEPHB4, or EFNB2-OE treated with NVP-BHG712. Scale bar: 25 μm. **d.** Experimental liver metastasis established by splenic inoculation of SW480Luc cells modified with empty vector, EFNB2-OE, EFNB2-OE + siEPHB4, or EFNB2-OE + NVP-BHG712 (n = 6 animals/group). Progression tracked via in vivo bioluminescence. Color scale: 2.81×10^6 to 4.40×10^7. **e.** Direct intrahepatic implantation model using similarly modified SW480Luc cells (n = 6/group). Tumor development monitored by bioluminescence imaging. Color scale: 2.50×10^7 to 4.55×10^8. **f.** PCNA detection via immunohistochemistry in metastatic liver tumors from the vector, EFNB2-OE, EFNB2-OE + siEPHB4, and EFNB2-OE + NVP-BHG712 cohorts. Scale bar: 50 μm. **g.** PCNA immunohistochemistry in tumors from the intrahepatic injection model across the same treatment groups. Scale bar: 50 μm. **h.** Procedure for enzymatic dissociation of liver metastases from vector-control or EFNB2-OE animals, followed by primary culture of recovered tumor cells. **i.** Growth assessment by CCK-8 in primary cultures of SW480 cells isolated from vector versus EFNB2-OE liver metastases. **j.** EdU proliferation assay in primary cultures of SW480 cells derived from vector versus EFNB2-OE metastatic lesions. Scale bar: 50 μm.

In vitro studies were replicated three times. Values shown as mean ± SD. Differences evaluated with Student's t-test. ns: not significant; *$p < 0.05$; **$p < 0.01$; ***$p < 0.001$.

EFNB2/EPHB4 signaling stimulates cholesterol import through control of LDLR levels

To uncover how EFNB2/EPHB4 contributes to CRC liver metastasis, we applied Gene Set Enrichment Analysis to CRC LM samples stratified by EFNB2 levels. Cholesterol homeostasis pathways were prominently enriched among genes elevated in the high-EFNB2 subset (**Figure 4a**), hinting at involvement of this pathway. Indeed, metastatic tissues expressing high EFNB2 contained more total cholesterol than low-expressors **(Table 1).** Overexpressing EFNB2 in models of splenic metastasis or direct liver seeding raised cholesterol content in tumor cells (**Figures 4b and 4c**), whereas EFNB2 knockdown lowered it (**Figure 4a**). Disrupting EPHB4 function with siRNA or NVP-BHG712 abolished the cholesterol elevation triggered by EFNB2 (**Figures 4b and 4c**).

Cross-dataset examination of liver metastases versus primary CRC (GSE6988, GSE35834, GSE49355) showed reduced expression of cholesterol biosynthesis enzymes (HMGCS1, HMGCR, MSMO1, DHCR24) alongside increased levels of import-related receptors (LDLR, VLDLR, SCARB1) (**Figures 4b–h**). Notably, the liver environment is cholesterol-rich compared to colorectum or lung [17].

Culturing SW480 and HT29 cells in standard 10% FBS medium revealed EFNB2/EPHB4-dependent cholesterol accumulation, an effect largely lost in serum-free media **(Figures 4d and 4e).** In GSE6988 liver metastases, EFNB2 transcript levels correlated positively with import receptors (LDLR, VLDLR, SCARB1) **(Figure 5a)** but showed no association with biosynthetic genes (HMGCS1, HMGCR, NSDHL, MSMO1, DHCR24) **(Figure 5b).**

Within metastasis models, EFNB2 gain-of-function boosted LDLR while leaving synthesis genes unchanged **(Figure 4f)**; loss-of-function had the opposite effect on LDLR **(Figure 5c).** Interfering with EPHB4 prevented EFNB2-induced LDLR elevation **(Figure 4f).** Remarkably, LDLR induction by this axis persisted even in serum-free cultures lacking exogenous cholesterol **(Figures 4g and 5d).** Supplying external cholesterol lowered intracellular stores after EFNB2 depletion **(Figure 4h),** and EPHB4 inhibition blocked EFNB2-mediated cholesterol buildup under lipid-deprived conditions **(Figure 4i).**

In summary, EFNB2 engagement of EPHB4 enhances cholesterol acquisition in CRC liver metastases predominantly by driving LDLR expression.

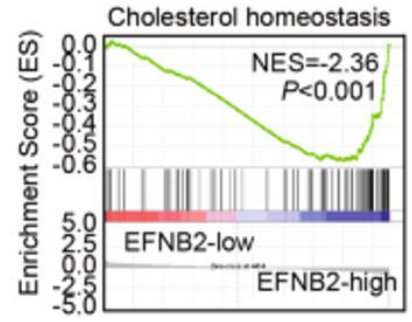

a)

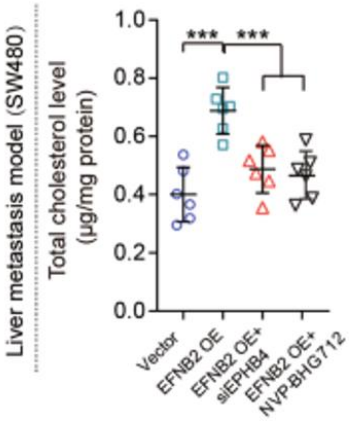

b)

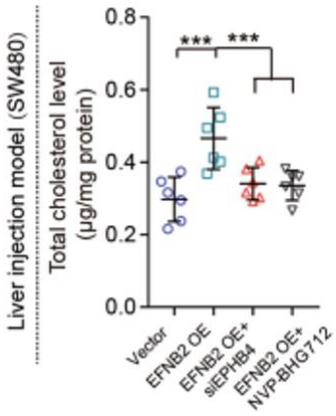

c)

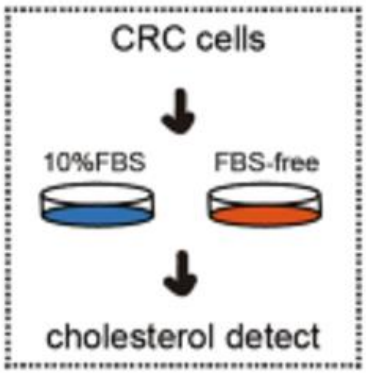

d)

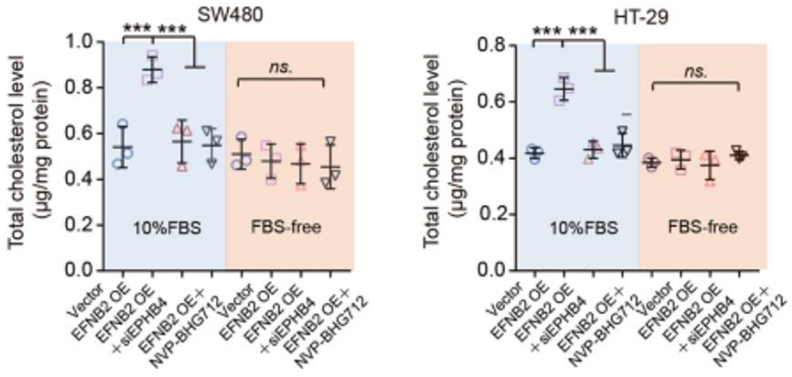

e)

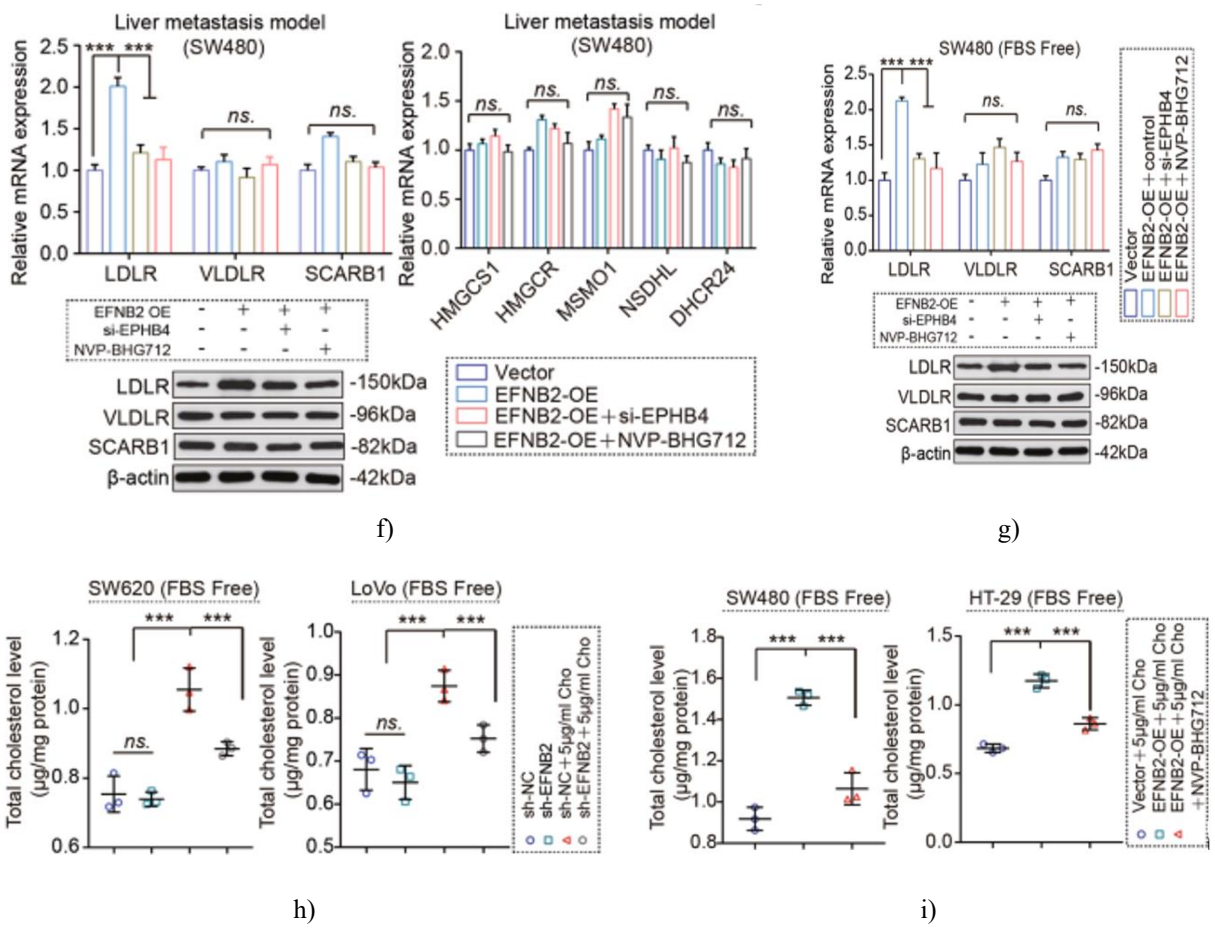

Figure 4. EFNB2/EPHB4 signaling enhances cholesterol import through upregulation of LDLR.

a. Gene Set Enrichment Analysis (GSEA) based on EFNB2 levels in colorectal cancer liver metastases from the GSE6988 dataset. The 24 samples were stratified into high-EFNB2 (n=12) and low-EFNB2 (n=12) groups. **b.** Quantification of total cholesterol in liver metastatic tumors from mice in the vector, EFNB2-OE + siEPHB4, EFNB2-OE, and EFNB2-OE + NVP-BHG712 groups (n=6 per group). **c.** Total cholesterol measurement in tumors from the direct intrahepatic injection model across the same groups as in B (n=6 per group). **d.** Assessment of intracellular cholesterol content in CRC cell lines. **e.** Cholesterol levels in HT29 and SW480 cells expressing vector, EFNB2-OE + siEPHB4, EFNB2-OE, or EFNB2-OE + NVP-BHG712, cultured with or without 10% FBS supplementation. **f.** mRNA expression of cholesterol import-associated genes (VLDLR, LDLR, SCARB1) and biosynthesis-associated genes (DHCR24, HMGCR, NSDHL, HMGCS1, MSMO1) in metastatic liver tumors from the vector, EFNB2-OE + siEPHB4, and EFNB2-OE + NVP-BHG712, EFNB2-OEgroups (n=6 per group). **g.** Expression profiles of the same cholesterol import and biosynthesis genes in SW480 cells maintained in serum-free medium, across the vector, EFNB2-OE + siEPHB4, EFNB2-OE, and EFNB2-OE + NVP-BHG712 conditions. **h.** Intracellular cholesterol levels in LoVo and SW620cells cultured serum-free, comparing sh-EFNB2, sh-NC, sh-NC + 5 μg/ml cholesterol, and sh-EFNB2 + 5 μg/ml cholesterol treatments. **i.** Cholesterol content in SW480 and HT29 cells under serum-free conditions with 5 μg/ml cholesterol supplementation, in vector, EFNB2-OE + NVP-BHG712 and EFNB2-OE groups.

All in vitro experiments were replicated three times. Data are shown as mean ± SD. Statistical analysis was performed using Student's t-tests. ns: no significant difference; ***$p < 0.001$.

EFNB2/EPHB4 signaling drives LDLR transcription via STAT3 activation

To elucidate how EPHB4/EFNB2 controls LDLR expression, we first examined known regulators of cholesterol metabolism. Although Sterol-Regulatory Element-Binding Protein 2 (SREBP2) is a key transcription factor in cholesterol homeostasis [18], EPHB4/ EFNB2 activation had no impact on SREBP2 expression or processing **(Figure 5a).**

Bioinformatic prediction of transcription factors binding to LDLR and cholesterol synthesis genes identified Signal Transducer and Activator of Transcription 3 (STAT3) as a candidate that specifically targets the LDLR promoter, but not promoters of synthesis-related genes **(Figure 5b).** Functional assays confirmed direct binding of STAT3 to the LDLR promoter and its ability to enhance LDLR transcription (**Figures 5c and d).** Mutating the STAT3 binding site eliminated this transcriptional activation **(Figure 5d).**

Knockdown of STAT3 with siRNA or treatment with the selective inhibitor SH-4-54 reduced LDLR levels in CRC cells **(Figure 5e).** Canonical STAT3 signaling involves phosphorylation by receptor-associated kinases, followed by dimerization, nuclear translocation, and target gene activation. Consistent with this, EPHB4/ EFNB2 engagement increased phosphorylation of JAK2 and STAT3 **(Figures 5f and g).** Importantly, inhibiting STAT3 abrogated the LDLR induction mediated by EPHB4/ EFNB2 **(Figure 5h).**

These findings indicate that EPHB4/EFNB2 promotes LDLR transcription predominantly through activation of the STAT3/JAK2 pathway.

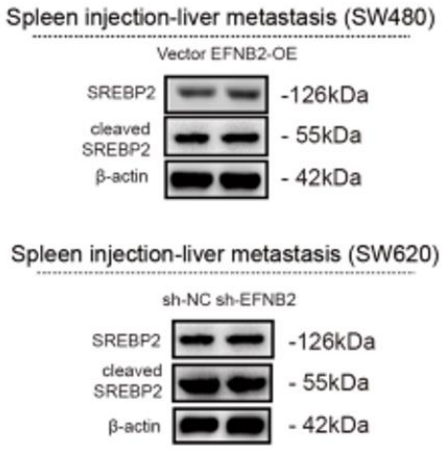

a)

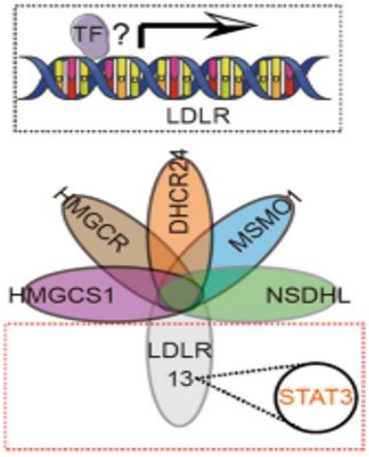

b)

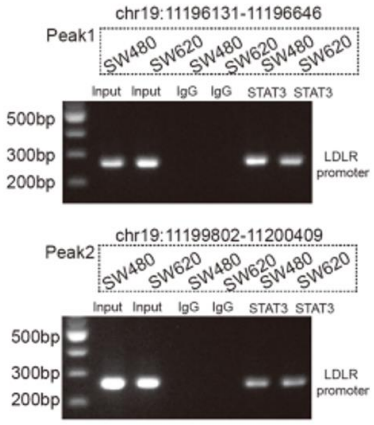

c)

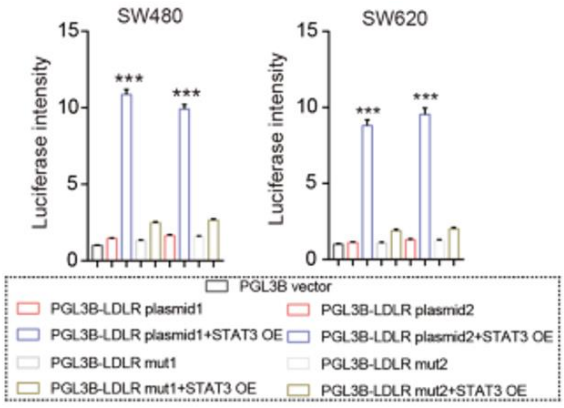

d)

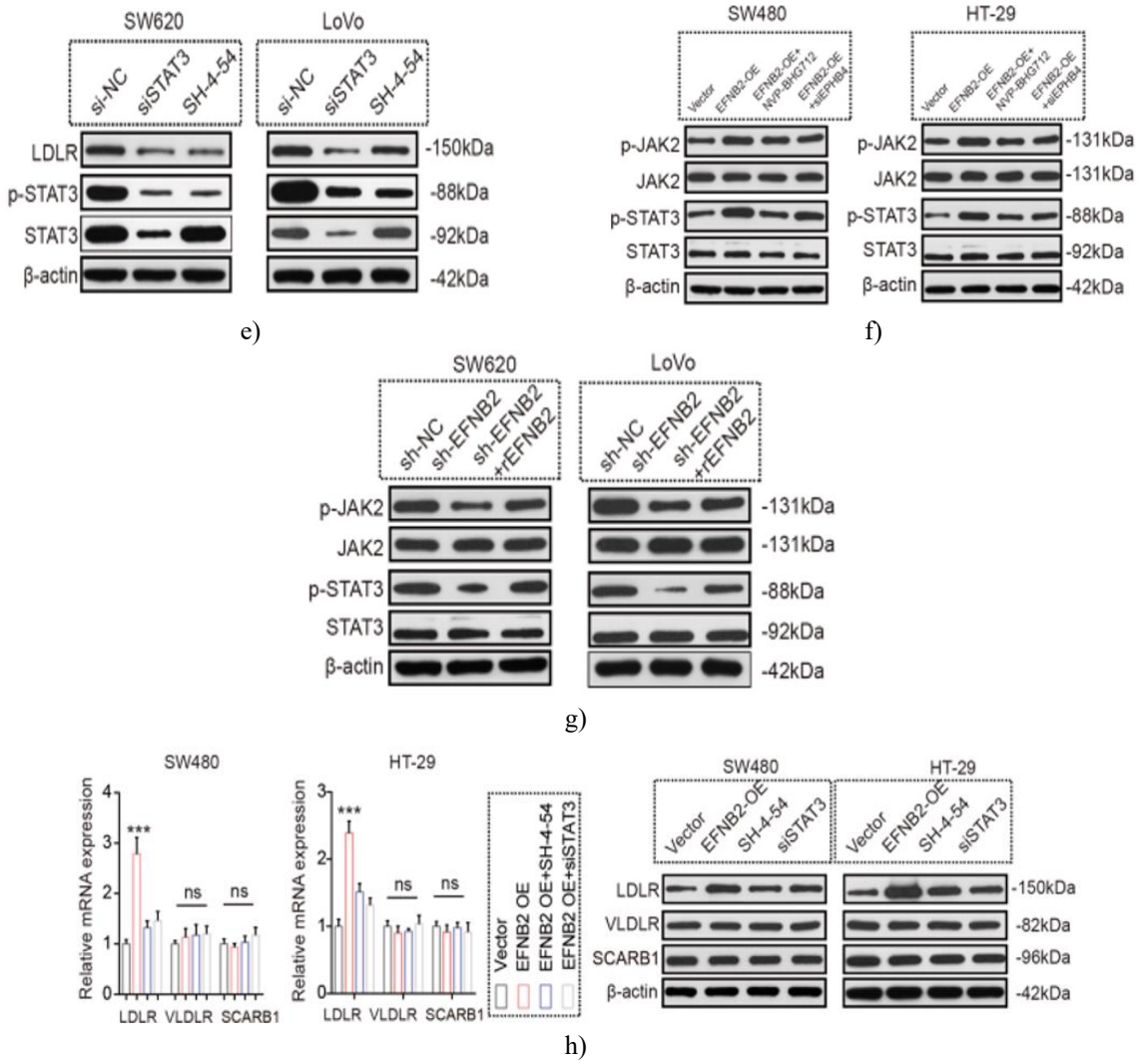

Figure 5. EFNB2/EPHB4 Axis Enhances LDLR Transcription via STAT3

a. The protein levels of total and activated SREBP2 were assessed in CRC liver metastasis (LM) tissues transfected with either a control vector or EFNB2 overexpression (EFNB2-OE) (n = 6). **b.** Analysis of transcription factors regulating LDLR expression was performed. **c.** Chromatin immunoprecipitation (ChIP) assays confirmed that STAT3 binds to the LDLR promoter in SW480 and SW620 cells. **d.** Dual luciferase reporter assays demonstrated that STAT3 promotes LDLR transcription. **e.** Protein expression of LDLR, STAT3, and phosphorylated STAT3 (p-STAT3) was examined in SW620 and LoVo cells treated with si-NC, siSTAT3, or the STAT3 inhibitor SH-4-54. **f.** In SW480 and HT29 cells, EFNB2 overexpression increased JAK2 and STAT3 phosphorylation, which was reversed by treatment with NVP-BHG712 or siEPHB4. **g.** In SW620 and LoVo cells, knockdown of EFNB2 (sh-EFNB2) reduced JAK2 and STAT3 phosphorylation, and this effect was rescued by recombinant EFNB2 (rEFNB2). **h.** mRNA and protein levels of LDLR, VLDLR, and SCARB1 were elevated upon EFNB2 overexpression in SW480 and HT29 cells, while inhibition of STAT3 (via SH-4-54 or siSTAT3) blocked these effects.

All experiments were conducted in triplicate, and data are expressed as mean ± SD. Statistical significance was determined by Student's t-tests, with "ns" indicating no significant difference and ***$p < 0.001$.

LDLR is essential for EFNB2/EPHB4-Mediated CRC liver metastasis growth

While the EFNB2/EPHB4 axis was shown to transcriptionally regulate LDLR, it remained unclear

whether LDLR contributes to the axis's tumor-promoting effects in CRC LM.

In vivo studies revealed that LDLR knockdown by siRNA blocked the tumor-promoting effect of EFNB2 overexpression in liver metastatic CRC.

Inhibition of LDLR also reversed the EFNB2-induced upregulation of PCNA, a marker of proliferation.

Although LDLR mediates the contribution of EFNB2/EPHB4 to CRC LM, it was uncertain whether LDLR-driven cholesterol uptake is involved.

Both in vivo and in vitro experiments showed that blocking LDLR reversed EFNB2/EPHB4-induced cholesterol accumulation.

Supplementing cells with exogenous cholesterol promoted survival in CRC cells cultured in serum-free medium, but this effect was completely blocked when LDLR was silenced. Additionally, inhibition of the EFNB2/EPHB4 axis suppressed the pro-survival effects under cholesterol treatment.

Thus, the EFNB2/EPHB4 axis promotes CRC liver metastasis growth primarily through LDLR-mediated cholesterol uptake, highlighting LDLR as a key downstream effector of EFNB2/EPHB4 signaling.

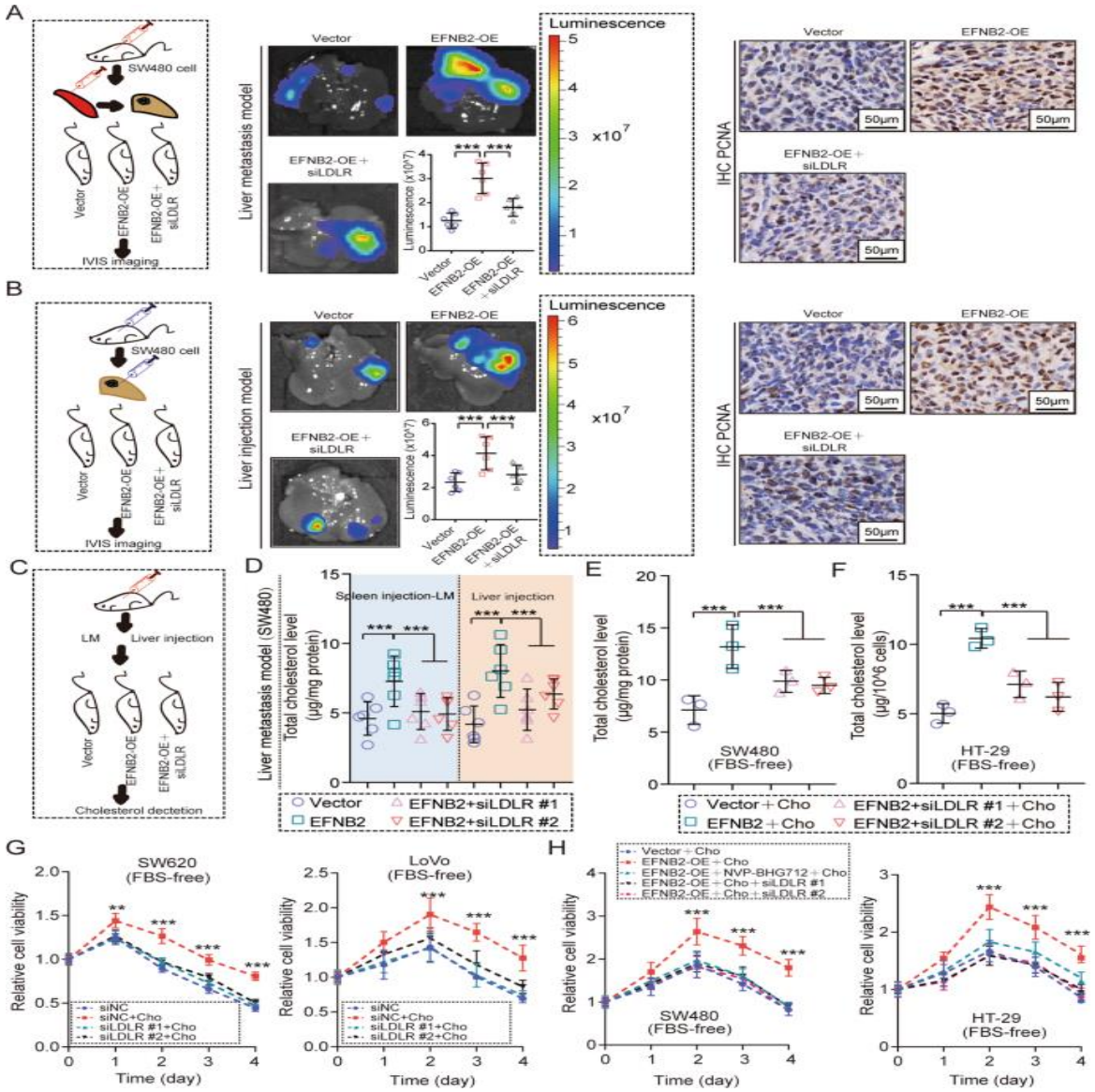

Figure 6. LDLR Is Required for EFNB2/EPHB4-Mediated CRC Liver Metastasis

A. To evaluate the role of LDLR in EFNB2-driven liver metastasis, SW480^luc cells transfected with vector, EFNB2 overexpression (EFNB2-OE), or EFNB2-OE combined with either siLDLR #1 or siLDLR #2 were injected into the spleens of mice (n = 6 per group). Tumor growth was monitored through in vivo imaging, and proliferation in tumor tissues was assessed by PCNA immunohistochemistry. Scale bar: 50 μm. **B.** A similar experimental setup was used in a liver injection model, where tumor progression and PCNA expression were measured under the same transfection conditions (n = 6 per group). Scale bar: 50 μm. **C–D.** Cholesterol content was quantified in tumors from both the spleen and liver injection models. EFNB2-OE increased cholesterol accumulation, which was reversed when LDLR was silenced (siLDLR #1 or #2) (n = 6 per group). **E–F.** In SW480 and HT29 cells cultured in serum-free medium or treated with exogenous cholesterol (5 μg/ml), EFNB2 overexpression raised intracellular cholesterol levels. Knockdown of LDLR prevented this increase, confirming LDLR's role in cholesterol uptake. **G–H.** Cell viability assays (CCK-8) showed that exogenous cholesterol promoted survival of SW620, LoVo, SW480, and HT29 cells under serum-free conditions. Silencing LDLR or blocking the EFNB2/EPHB4 pathway inhibited this survival advantage, indicating that EFNB2/EPHB4 enhances cell survival through LDLR-dependent cholesterol uptake.

All experiments were performed in triplicate. Data are presented as mean ± SD. Statistical significance was determined using Student's t-tests, with ns indicating no significance, **p < 0.01, and ***p < 0.001.

EFNB2/EPHB4 as a therapeutic target in CRC liver metastasis

Analysis of patient data revealed that elevated EFNB2 expression in CRC liver metastases is associated with shorter overall survival compared to low EFNB2 expression **(Figures 7a).**

Because the liver is a key organ for cholesterol metabolism, a high-cholesterol diet model in BALB/c nude mice was established. Mice fed a high-cholesterol diet had significantly higher liver cholesterol than those on a normal diet (**Figures 7b–c**).

The study demonstrated that aberrant EFNB2/EPHB4 activation promotes LDLR-mediated cholesterol uptake. This prompted investigation into whether targeting this axis could improve survival. In a liver metastasis model **(Figure 7d)**, mice on a high-cholesterol diet exhibited reduced survival relative to normal-diet mice **(Figure 7e).**

Importantly, inhibiting the EFNB2/EPHB4 axis markedly extended survival, even under a high-cholesterol diet, underscoring its central role in controlling cholesterol uptake and tumor progression **(Figure 7e).**

In conclusion, metastatic CRC cells with overactive EFNB2/EPHB4 exploit extracellular cholesterol in the liver to support colonization and tumor growth, highlighting EFNB2/EPHB4 as a promising therapeutic target **(Figure 7f).**

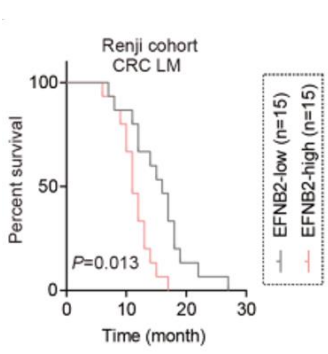

a)

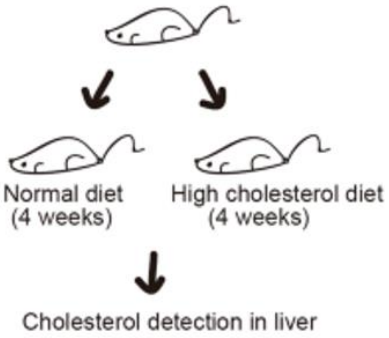

b)

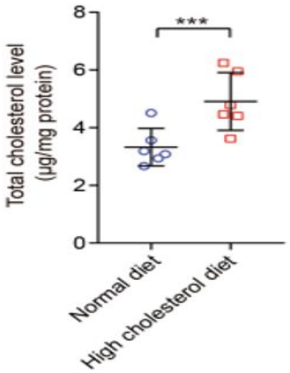

c)

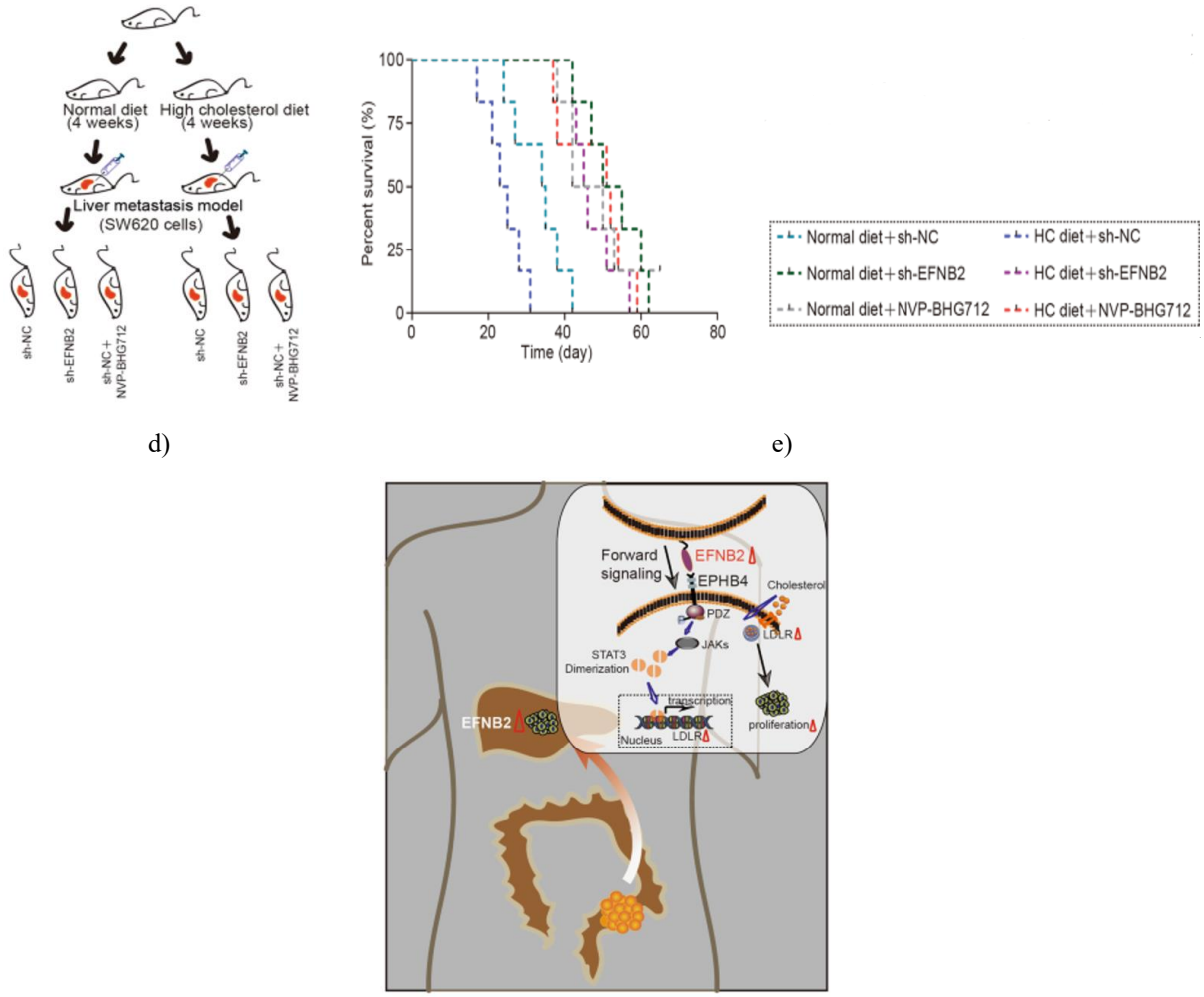

d) e) f)

Figure 7. EFNB2/EPHB4 Axis as a Therapeutic Target in CRC Liver Metastasis (LM)

a. Overall survival analysis of patients with CRC liver metastases was conducted according to EFNB2 protein expression (n = 30). **b–c.** A high-cholesterol mouse model was established by feeding BALB/c nude mice a cholesterol-rich diet. Liver cholesterol levels were measured, showing significantly higher levels in the high-cholesterol group compared to controls (n = 6 per group). **d–e.** CRC liver metastasis models were generated using SW620 cells in mice under high-cholesterol and normal diets, with groups including sh-NC, sh-EFNB2, and sh-NC treated with NVP-BHG712 (n = 6 per group). Overall survival analysis revealed that EFNB2 knockdown or inhibition of the EFNB2/EPHB4 axis improved survival, even under a high-cholesterol diet. **f.** Mechanistically, adaptive activation of the EFNB2/EPHB4 axis enhances CRC liver metastasis through LDLR-mediated cholesterol uptake.

All experiments were performed in triplicate. Data are presented as mean ± SD, and statistical significance was assessed using Student's t-tests (***$p < 0.001$).

Metastatic tumor cells exhibit distinct expression profiles in different organ environments due to structural and metabolic differences, highlighting the necessity for genetic adaptation to the metastatic microenvironment [6]. In this study, EFNB2 was found to be upregulated specifically in CRC liver metastases (LM), but not in primary colorectal tumors or peritoneal metastases (PM). Elevated EFNB2 contributed to post-metastatic tumor growth in the liver, suggesting a strong link between EFNB2 expression and hepatic tumor progression.

Ephrins are classified into two subgroups: Ephrin A and Ephrin B. Ephrins-EPHs signaling is highly complex and can operate through classic forward signaling (ligand-to-receptor), reverse signaling (receptor-to-ligand), or

bidirectional signaling [19]. Previous studies showed that (1) EFNB2 overexpression strongly promotes post-metastatic CRC LM growth, and (2) blocking EFNB2 forward signaling—but not reverse signaling—suppresses its tumor-promoting effects. This indicates that EFNB2 primarily acts through forward signaling in CRC LM.

EPHs, the classical receptors of Ephrins, are divided into EPHA and EPHB classes. Typically, Ephrin A ligands bind EPHA receptors, while Ephrin B ligands bind EPHB receptors, though Ephrin B can also interact with EPHA4 [11]. EFNB2 has been reported to drive tumor progression in pancreatic ductal adenocarcinoma, breast cancer, and glioblastoma [20-22]. Moreover, inhibiting EFNB2/EPHB4 signaling increased sensitivity to cetuximab-radiotherapy in head and neck cancer [23]. In CRC LM, EFNB2 enhanced proliferation by engaging EPHB4, and blocking EPHB4 abolished this effect.

The liver serves as the central organ for cholesterol metabolism [24], producing approximately 80% of the body's cholesterol, which is subsequently converted into steroid hormones and bile acids, creating a cholesterol-rich microenvironment [25]. Cholesterol is a vital component of cellular and organelle membranes [26], and rapidly proliferating cancer cells require increased cholesterol for membrane biogenesis [27, 28]. Our study found that the EFNB2/EPHB4 axis elevated total cholesterol levels in CRC LM.

Intracellular cholesterol is derived from both endogenous synthesis and extracellular uptake [29]. Bioinformatics analysis and experimental models demonstrated that EFNB2/EPHB4 increased LDLR expression without affecting genes responsible for cholesterol synthesis. LDLR is the primary receptor mediating cholesterol uptake [30], enabling extracellular lipoprotein-cholesterol complexes to enter cells via endocytosis, where lysosomal enzymes release free cholesterol for cellular functions [31]. In CRC cells cultured in FBS-free medium, removal of exogenous cholesterol abolished the EFNB2/EPHB4-mediated increase in cholesterol, whereas supplementation with exogenous cholesterol enhanced it.

Sterol regulatory element-binding protein 2 (SREBP2) is an intracellular cholesterol sensor located in the endoplasmic reticulum that regulates cholesterol homeostasis via the Insig-SREBP-SCAP pathway [32]. However, EFNB2/EPHB4 did not alter SREBP2 expression or activation in CRC LM. Data analysis and experimental validation revealed that STAT3 can transcriptionally activate LDLR. Phosphorylated STAT3 forms homo- or heterodimers that translocate to the nucleus and bind promoter regions to initiate gene transcription [33]. Eph receptors, as tyrosine kinases, can activate downstream pathways through phosphorylation. For instance, EPHB2 induces STAT3 phosphorylation to promote angiogenesis [34], and EPHA4 activates the JAK/STAT3 pathway [35]. In this study, EFNB2/EPHB4 enhanced STAT3 phosphorylation, while STAT3 inhibition significantly reduced LDLR upregulation, demonstrating that LDLR mediates EFNB2/EPHB4 effects on intracellular cholesterol and CRC LM growth.

Clinical and preclinical evidence indicates that hypercholesterolemia promotes metastatic tumor progression [36]. High-cholesterol diets have been shown to increase liver metastasis burden in melanoma models [37]. Consistently, mice with CRC LM fed a high-cholesterol diet exhibited shorter survival, whereas EFNB2/EPHB4 inhibition markedly prolonged survival, even under high-cholesterol conditions.

Despite these findings, some limitations remain: (1) the CRC LM sample size was limited, reducing clinical analysis robustness; (2) the translational potential of targeting EFNB2/EPHB4 in CRC LM requires further validation; and (3) alternative mechanisms by which EFNB2/EPHB4 regulates LDLR are not fully understood. Nonetheless, this study identifies a specific role for EFNB2/EPHB4 in CRC LM progression, offering a potential therapeutic strategy for patients with hepatic metastases.

Materials and Methods

Specimen collection and patient enrollment

A total of 30 cases, comprising colorectal cancer (CRC) primary tumor tissues, matched adjacent non-tumorous tissues, and corresponding liver metastasis tissues, were obtained from patients treated at the Department of Gastrointestinal Surgery, Renji Hospital, Shanghai Jiao Tong University School of Medicine. These specimens were collected from CRC patients who underwent surgical resection at the same department between January 2014 and January 2019. The criteria for patient inclusion and exclusion are described in the supplementary materials and methods section.

Tissue sample acquisition

Immediately following surgical resection, CRC tumor tissues and paired noncancerous tissues were promptly harvested from the surgical specimens. Tumor samples

were taken from viable regions showing no obvious necrosis, while noncancerous samples were collected at least 5 cm distant from the tumor edge. All tissues were placed individually into Eppendorf tubes and snap-frozen in liquid nitrogen for storage.

Cell-based experiments

Inhibitors and reagents

Cholesterol (catalog no. C3045) was acquired from Sigma-Aldrich (St. Louis, MO, USA) and prepared in absolute ethanol for use in cellular assays. NVP-BHG712 (50 mg) was obtained from Selleck Chemicals (Houston, TX, USA) and solubilized in DMSO. For in vitro studies, a concentration of 25 nM was applied, whereas in vivo mouse experiments involved oral administration at a dose of 3 mg/kg. The STAT3 inhibitor SH-4-54 was also purchased from Selleck Chemicals, dissolved in DMSO, and used at a concentration of 150 nM in cell-based experiments.

Cell culture

The colorectal cancer (CRC) cell lines employed in this study—SW620, LoVo, SW480, HT29, RKO, and HCT-116 (all human CRC-derived)—as well as the normal colonic epithelial cell line NCM460, were sourced from and authenticated by the Cell Bank of the Chinese Academy of Sciences (Shanghai, China). All cell lines were maintained in Dulbecco's Modified Eagle's Medium (DMEM) containing 10% fetal bovine serum (FBS) and 1% penicillin-streptomycin. Cultures were incubated at 37°C in a humidified incubator with 5% CO_2.

Small Interfering RNA (siRNA) transfection

siRNAs targeting EPHB2, EPHB1, EPHB4, EPHB3, EPHB6, EPHB5, and EPHA4 were acquired from Shanghai GenePharma Co., Ltd. (Shanghai, China). Transfection procedures followed previously established protocols [38], with detailed methods provided in the Supplementary Materials and Methods.

Lentiviral transduction

Full-length human EFNB2 cDNA was introduced into CRC cell lines via lentiviral vectors to create stable EFNB2-overexpressing cells (Lentivirus-EFNB2; denoted EFNB2-OE). Constructs encoding truncated variants of EFNB2—including a C-terminal deletion (ΔC EFNB2), a C-terminal deletion with His-tag (ΔC + H EFNB2), and an extracellular domain-only version (ΔE EFNB2)—were also generated. An empty lentiviral vector (Lentivirus-NC) served as the negative control. For knockdown experiments, a short hairpin RNA (shRNA) targeting EFNB2 was delivered lentivirally to produce sh-EFNB2 cells, with a non-targeting shRNA (sh-NC) as the control. Lentiviral constructs were supplied by Shanghai GenePharma Co., Ltd. (Shanghai, China).

Real-Time Quantitative Polymerase Chain Reaction (RT-qPCR)

Total RNA was isolated using TRIzol reagent, followed by reverse transcription into cDNA with the PrimeScript™ Kit (Takara Bio Inc., Shiga, Japan). Expression levels were normalized to 18S rRNA as an endogenous control. Target gene expression was quantified using the $^{-\Delta}$Ct or $^{-\Delta\Delta}$Ct method.

Western blotting

Whole-cell protein lysates were prepared, and protein concentrations were determined using the BCA assay. Western blot procedures were conducted as previously reported [38]. Primary antibodies included: EPHB4 (ab150545 and ab98933, Abcam), EFNB2 (ab69858, Abcam, Cambridge, UK), β-catenin (ab32572, Abcam), LDLR (ab52818, Abcam), SCARB1 (ab52629, Abcam), STAT3 (ab68153, Abcam), phosphorylated STAT3 (ab267373, Abcam), VLDLR (ab203271, Abcam), phosphorylated JAK2 (ab108596, Abcam), JAK2 (ab108596, Abcam), SREBP2 (ab30682, Abcam), and proliferating cell nuclear antigen (PCNA; Proteintech Group, Inc., Sankt Leon-Rot, Germany). Secondary antibodies were horseradish peroxidase (HRP)-conjugated HRP-conjugated Affinipure Goat Anti-Mouse IgG (H + L) (SA00001-1) and Affinipure Goat Anti-Rabbit IgG (H + L) (SA00001-2), both from Proteintech Group, Inc. (Chicago, USA).

Immunohistochemistry

Tissue specimens were embedded in paraffin and sectioned at a thickness of 4 μm. Sections were deparaffinized in xylene and rehydrated through a graded ethanol series. Antigen retrieval was performed using sodium citrate buffer, followed by quenching of endogenous peroxidase activity with 0.3% hydrogen peroxide (H_2O_2). Non-specific binding sites were blocked with bovine serum albumin. Sections were then sequentially incubated with primary and secondary antibodies. Color development was achieved using 3,3′-

diaminobenzidine (DAB) kits (ab64238, Abcam), and nuclei were counterstained with hematoxylin. Finally, sections were dehydrated in ethanol gradients and mounted with neutral resin. IHC staining intensity was scored according to pixel-based evaluation: 1 for no staining, 2 for weak, 3 for moderate, and 4 for strong staining.

Cholesterol quantification

Intracellular and tissue cholesterol levels in CRC cells and liver metastases were measured using Cholesterol/Cholesteryl Ester Quantitation Assay kits (ab65359, Abcam). For analysis, either 10^6 CRC cells or 10 mg of metastatic liver tissue were processed according to the kit protocol.

Luciferase reporter assay

Plasmids overexpressing STAT3 were introduced into CRC cells using Roche X-tremeGENE HP DNA Transfection Reagent (Roche Diagnostics, Basel, Switzerland). Corresponding luciferase reporter constructs were co-transfected in each experimental group. Cells were subsequently treated with Dual-Glo Luciferase Reagent, and luminescence signals were quantified on a SpectraMax M5 plate reader using the Dual-Glo Luciferase Assay system.

Chromatin immunoprecipitation **(***ChIP) PCR assay*

ChIP experiments were performed with the Pierce™ Agarose ChIP Kit (26156, Thermo Fisher Scientific, Waltham, MA, USA). CRC cells were crosslinked with 1% formaldehyde, and crosslinking was terminated by addition of glycine. Chromatin was digested into fragments using Micrococcal Nuclease in MNase Digestion Buffer. Aliquots of fragmented chromatin were immunoprecipitated overnight with antibodies against STAT3, IgG (negative control), or RNA polymerase II (positive control). Immunocomplexes were captured, washed, and eluted, followed by DNA purification. Enriched DNA fragments were analyzed by PCR to confirm binding.

In vivo experiments

Mice were randomly allocated to experimental groups, and animal studies were conducted in a blinded manner. All procedures were approved by the Research Ethics Committee of Renji Hospital and complied with institutional and national guidelines for the ethical use and care of laboratory animals. Detailed protocols are provided in the Supplementary Materials and Methods.

Isolation and ex vivo culture of liver metastasis cells

Liver metastatic tissues were harvested from mice in the splenic injection metastasis model and minced into approximately 2 mm pieces. Tissues were enzymatically dissociated using collagenase/hyaluronidase supplemented with DNase I. Digestion was carried out at 37°C for 30 minutes. The resulting suspension was passed through cell strainers to obtain single-cell preparations. Isolated metastatic cells were then maintained in DMEM medium containing 10% FBS and 1% penicillin-streptomycin.

Statistical analysis

All quantitative measurements are reported as mean ± standard deviation (SD). Statistical processing was conducted using SPSS 20.0 (Chicago, IL, USA) and GraphPad Prism 7 (GraphPad Software, San Diego, CA, USA; www.graphpad.com).

To evaluate the relationship between EFNB2 expression and clinical features in CRC patients, either chi-square tests or independent-sample t-tests were applied depending on the data type. Continuous variables, such as patient age or tumor size, were compared using t-tests, while categorical and ordinal variables—including sex, tumor T stage, lymph node status, and presence of distant metastasis—were analyzed via chi-square tests. Correlations between two ranked variables were assessed using Spearman's rank correlation.

Survival outcomes were assessed by constructing Kaplan–Meier curves, and statistical differences between groups were evaluated using the log-rank test. A two-sided p-value < 0.05 was considered indicative of statistical significance.

Acknowledgments: None

Conflict of Interest: None

Financial Support: This study was supported by the National Natural Science Foundation of China (82072671) and Research Fund for medical engineering cross project of Shanghai Jiao Tong University (ZH2018ZDA08).

Ethics Statement: None

References

1. Li J, Yuan Y, Yang F, Wang Y, Zhu X, Wang Z, et al. Expert consensus on multidisciplinary therapy of colorectal cancer with lung metastases (2019 edition). J Hematol Oncol. 2019;12:16.
2. Chandra R, Karalis JD, Liu C, Murimwa GZ, Voth Park J, Heid CA, et al. The colorectal cancer tumor microenvironment and its impact on liver and lung metastasis. Cancers. 2021;13:6206.
3. Wei Q, Qian Y, Yu J, Wong CC. Metabolic rewiring in the promotion of cancer metastasis: mechanisms and therapeutic implications. Oncogene. 2020;39:6139–56.
4. Bergers G, Fendt SM. The metabolism of cancer cells during metastasis. Nat Rev Cancer. 2021;21:162–80.
5. Dupuy F, Tabaries S, Andrzejewski S, Dong Z, Blagih J, Annis MG, et al. PDK1-dependent metabolic reprogramming dictates metastatic potential in breast cancer. Cell Metab. 2015;22:577–89.
6. Bu P, Chen KY, Xiang K, Johnson C, Crown SB, Rakhilin N, et al. Aldolase B-mediated fructose metabolism drives metabolic reprogramming of colon cancer liver metastasis. Cell Metab. 2018;27:1249–62.e4
7. Ganesh K, Massague J. Targeting metastatic cancer. Nat Med. 2021;27:34–44.
8. Tsilimigras DI, Brodt P, Clavien PA, Muschel RJ, D'Angelica MI, Endo I, et al. Liver metastases. Nat Rev Dis Prim. 2021;7:27.
9. Bertocchi A, Carloni S, Ravenda PS, Bertalot G, Spadoni I, Lo Cascio A, et al. Gut vascular barrier impairment leads to intestinal bacteria dissemination and colorectal cancer metastasis to liver. Cancer Cell. 2021;39:708–24. e11
10. Zhang XL, Hu LP, Yang Q, Qin WT, Wang X, Xu CJ, et al. CTHRC1 promotes liver metastasis by reshaping infiltrated macrophages through physical interactions with TGF-beta receptors in colorectal cancer. Oncogene. 2021;40:3959–73.
11. Van Battum EY, Brignani S, Pasterkamp RJ. Axon guidance proteins in neurological disorders. Lancet Neurol. 2015;14:532–46.
12. Chedotal A. Roles of axon guidance molecules in neuronal wiring in the developing spinal cord. Nat Rev Neurosci. 2019;20:380–96.
13. Baeriswyl T, Dumoulin A, Schaettin M, Tsapara G, Niederkofler V, Helbling D, et al. Endoglycan plays a role in axon guidance by modulating cell adhesion. eLife 2021;10:e64767.
14. Neufeld G, Mumblat Y, Smolkin T, Toledano S, Nir-Zvi I, Ziv K, et al. The semaphorins and their receptors as modulators of tumor progression. Drug Resist Updat. 2016;29:1–12.
15. Jurcak NR, Rucki AA, Muth S, Thompson E, Sharma R, Ding D, et al. Axon guidance molecules promote perineural invasion and metastasis of orthotopic pancreatic tumors in mice. Gastroenterology. 2019;157:838–50.e6
16. Koohini Z, Koohini Z, Teimourian S. Slit/Robo signaling pathway in cancer; a new stand point for cancer treatment. Pathol Oncol Res. 2019;25:1285–93.
17. Minniti ME, Pedrelli M, Vedin LL, Delbes AS, Denis RGP, Oorni K, et al. Insights from liver-humanized mice on cholesterol lipoprotein metabolism and LXR-agonist pharmacodynamics in humans. Hepatology. 2020;72:656–70.
18. Yang HX, Zhang M, Long SY, Tuo QH, Tian Y, Chen JX, et al. Cholesterol in LDL receptor recycling and degradation. Clin Chim Acta. 2020;500:81–6.
19. Kania A, Klein R. Mechanisms of ephrin-Eph signalling in development, physiology and disease. Nat Rev Mol Cell Biol. 2016;17:240–56.
20. Bhatia S, Bukkapatnam S, Van Court B, Phan A, Oweida A, Gadwa J, et al. The effects of ephrinB2 signaling on proliferation and invasion in glioblastoma multiforme. Mol Carcinogenesis. 2020;59:1064–75.
21. Zhu F, Dai SN, Xu DL, Hou CQ, Liu TT, Chen QY, et al. EFNB2 facilitates cell proliferation, migration, and invasion in pancreatic ductal adenocarcinoma via the p53/p21 pathway and EMT. Biomedicine Pharmacother. 2020;125:109972.
22. Magic Z, Sandstrom J, Perez-Tenorio G. EphrinB2 inhibits cell proliferation and motility in vitro and predicts longer metastasisfree survival in breast cancer. Int J Oncol. 2019;55:1275–86.
23. Bhatia S, Sharma J, Bukkapatnam S, Oweida A, Lennon S, Phan A, et al. Inhibition of EphB4-Ephrin-B2 signaling enhances response to cetuximab-radiation therapy in head and neck cancers. Clin Cancer Res. 2018;24:4539–50.

24. de Boer JF, Kuipers F, Groen AK. Cholesterol transport revisited: a new turbo mechanism to drive cholesterol excretion. Trends Endocrinol Metab. 2018;29:123–33.
25. Liu A, Wu Q, Guo J, Ares I, Rodriguez JL, Martinez-Larranaga MR, et al. Statins: Adverse reactions, oxidative stress and metabolic interactions. Pharmacol Ther. 2019;195:54–84.
26. Schoop V, Martello A, Eden ER, Hoglinger D. Cellular cholesterol and how to find it. Biochim Biophys Acta Mol Cell Biol Lipids. 2021;1866:158989.
27. Kopecka J, Trouillas P, Gasparovic AC, Gazzano E, Assaraf YG, Riganti C. Phospholipids and cholesterol: inducers of cancer multidrug resistance and therapeutic targets. Drug Resist Updat. 2020;49:100670.
28. Song X, Sun X, Oh SF, Wu M, Zhang Y, Zheng W, et al. Microbial bile acid metabolites modulate gut RORgamma(+) regulatory T cell homeostasis. Nature. 2020;577:410–5.
29. Luo J, Yang H, Song BL. Mechanisms and regulation of cholesterol homeostasis. Nat Rev Mol Cell Biol. 2020;21:225–45.
30. Wang J, Wang YS, Huang YP, Jiang CH, Gao M, Zheng X, et al. Gypenoside LVI improves hepatic LDL uptake by decreasing PCSK9 and upregulating LDLR expression. Phytomedicine. 2021;91:153688.
31. Vos DY, van de Sluis B. Function of the endolysosomal network in cholesterol homeostasis and metabolic-associated fatty liver disease (MAFLD). Mol Metab. 2021;50:101146.
32. Waku T, Hagiwara T, Tamura N, Atsumi Y, Urano Y, Suzuki M, et al. NRF3 upregulates gene expression in SREBP2-dependent mevalonate pathway with cholesterol uptake and lipogenesis inhibition. iScience. 2021;24:103180.
33. Lin WH, Chang YW, Hong MX, Hsu TC, Lee KC, Lin C, et al. STAT3 phosphorylation at Ser727 and Tyr705 differentially regulates the EMT-MET switch and cancer metastasis. Oncogene. 2021;40:791–805.
34. Sato S, Vasaikar S, Eskaros A, Kim Y, Lewis JS, Zhang B, et al. EPHB2 carried on small extracellular vesicles induces tumor angiogenesis via activation of ephrin reverse signaling. JCI insight. 2019;4:e132447.
35. Lai KO, Chen Y, Po HM, Lok KC, Gong K, Ip NY. Identification of the Jak/Stat proteins as novel downstream targets of EphA4 signaling in muscle: implications in the regulation of acetylcholinesterase expression. J Biol Chem. 2004;279:13383–92.
36. Liu W, Chakraborty B, Safi R, Kazmin D, Chang CY, McDonnell DP. Dysregulated cholesterol homeostasis results in resistance to ferroptosis increasing tumorigenicity and metastasis in cancer. Nat Commun. 2021;12:5103.
37. Sun X, Essalmani R, Day R, Khatib AM, Seidah NG, Prat A. Proprotein convertase subtilisin/kexin type 9 deficiency reduces melanoma metastasis in liver. Neoplasia. 2012;14:1122–31.
38. Xu C, Gu L, Kuerbanjiang M, Wen S, Xu Q, Xue H. Thrombospondin 2/Toll-like receptor 4 axis contributes to HIF-1alpha-derived glycolysis in colorectal cancer. Front Oncol. 2020;10:557730.